CHEMICAL ENGINEERING TRANSACTIONS
VOL. 103, 2023
A publication of AIDIC
The Italian Association of Chemical Engineering
Online at www.cetjournal.it
Guest Editors: Petar S. Varbanov, Panos Seferlis, Yee Van Fan, Athanasios Papadopoulos

**ISBN** 979-12-81206-02-1; **ISSN** 2283-9216
DOI: 10.3303/CET23103145

# Validation of the Coupled Heat and Moisture in the Soil for Underground Thermal Energy Storage Systems

Sheng Zhang[a,*], Paweł Ocłoń[a], Mehmet Yildirim[a], Petar Sabev Varbanov[b], Olga Arsenyeva[b], Petro Kapustenko[b]

[a]Energy Department, Faculty of Environmental and Energy Engineering, Cracow University of Technology, Al. Jana Pawła II 37, 31-864, Cracow, Poland
[b]Sustainable Process Integration Laboratory – SPIL, NETME Centre, Faculty of Mechanical Engineering, Brno University of Technology – VUT Brno, Technická 2896/2, 616 69 Brno, Czech Republic
sheng.zhang@doktorant.pk.edu.pl

The Renewable Energy System for Residential Building Heating and Electricity Production (RESHeat ) system is a typical application of the utilisation of sun-tracked Photovoltaic Thermal (PVT) panels and underground heat storage units. This work introduces a MATLAB simulation model coupled with moisture and heat transfer processes. Validation of the proposed model from experimental measurements was conducted. The simulations were performed for a single year of RESHeat system operation for demo sites located in Cracow City. Results showed that the relative error between calculation and measurement varies from 0.258 % to 5.829 %, along with the same temperature trend. A Control Volume method is used to simulate coupled heat transfer in the ground.

## 1. Introduction

Renewable Energy (RE) makes great contributions to the natural environment and sustainable development. It provides a solution for solving the problem of excessive emission of Greenhouse Gases (GHG) by large traditional fossil fuels consumption. Solar energy resource, as a promising and reliable alternative renewable, is widely used in the architectural and industrial sectors. However, the biggest obstacle in applying solar energy as a RE lies in the fact that there is a mismatch between the highest availability and highest demand influenced by the natural climatic condition. The Renewable Energy System for Residential Building Heating and Electricity Production (RESHeat) passes a novel, fully renewable energy source on integrating heating, cooling and electricity production with the Underground Heat Storage Unit (UHSU). The basic principle of the proposed system is using solar energy as a primary RE. A series of sun-tracked PVT panels and sun-tracked Solar Collectors (SCs) are arranged to generate heat and electricity for thermal utilisation and power generation. A ground source heat pump serves the heating and cooling of the building. The UHSU exemplifies the novelty of gathering thermal energy from the waste heat and excess heat from SCs and cooling processes of PVT during the summertime and delivers heat for Domestic Hot Water (DHW) use by the hot water storage tank (an insulated tank) whilst regenerating the ground soil to avoid the decrease of heat pump efficiency via a heat accumulator (a non-insulated tank) (Ocłoń et al., 2023).
Underground Heat Storage Units are widely recommended as an excellent approach for designing the energy framework in civic buildings. Ocłoń et al. (2020) investigated a model of the radiator used for PV panel cooling by the 3D control volume method. It is displayed that lowering the PV panel's temperature could increase the gross efficiency of sun-tracked PVT units. Ocłoń et al. (2021) introduced an optimisation method for a heat pump system coupled with the UHSU to obtain the maximum share of renewable energy sources. The Jaya algorithm could lead to a total of 93 % heat energy which was covered by utilising UHSUs. Xu et al. (2022) presented a cylindrical model of seasonal thermal storage systems with solar collectors. Daneshazarian et al. (2022) developed a two-step optimisation model to match the thermal storage medium (TSM) in UHSU for buildings. Zhang et al. (2022) provided a comprehensive review of the application of hybrid renewable energy systems in

Paper Received: 12 May 2023; Revised: 05 June 2023; Accepted: 18 June 2023
Please cite this article as: Zhang S., Ocłoń P., Yildirim M., Varbanov P.S., Arsenyeva O., Kapustenko P., 2023, Validation of the Coupled Heat and Moisture in the Soil for Underground Thermal Energy Storage Systems, Chemical Engineering Transactions, 103, 865-870 DOI:10.3303/CET23103145

buildings including PCM thermal energy storage. Li et al. (2023) developed a nearly net-carbon refrigeration approach with an underground cold storage unit. For the selected area, this promising system could fulfill the indoor cooling requirements and showed a great potential for future buildings own to the greener characteristic. This paper introduces a coupled moisture-heat model of an underground heat storage unit in RESHeat. The 2D model concerns solar-assisted ground resource heat pump, the PVT, solar collectors and UHSU which takes the influence of ground heat transfer into account. The simulations were performed for a single year of RESHeat system operation for demo sites located in Cracow City. A Control Volume method under the MATLAB platform is used to simulate coupled heat transfer in the ground. The coupled model is verified by the actual measurements of the demo site in Poland.

## 2. Mathematical model of the coupled model

The proposed heating system consists of sun-tracked PV panels and solar collectors, water type ground heat pump and an underground storage system (Figure 1). It utilises the thermal energy from PV panels cooling and SCs while waste heat and excess heat from PV panels and SCs is accumulated in the ground via the UHSU and returned for additional thermal energy preparation during heating seasons.

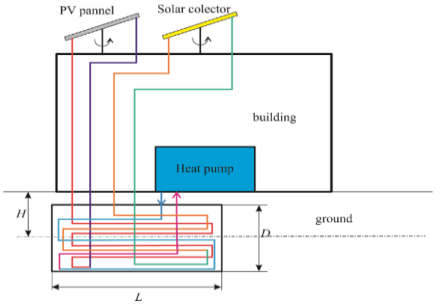


*Figure 1: Schematic description of the proposed design*

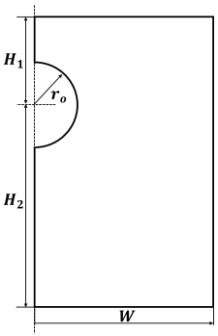


*Figure 2: Geometric scheme for calculation of the ground temperature*

The geometric of the underground heat storage tank is followed in Figure 2. It assumes the symmetrical partition for simplifying the heat transfer for the cross-section of the calculating domain. The tank burial depth $H_1$ is assumed as 5 m, and the width of the domain $W$ is assumed as 12 m. The total height of the domain $H_1 + H_2$ is 20 m. The outer radius of the tank is equal to 1.5 m. The mathematical model of underground tanks is developed in MATLAB. The Finite Volume Formulation is used for defining a ground domain with all the relevant boundary conditions. In Cracow, the yearly average ground temperature is set to 7.5 °C. With the symmetrical condition, the left side of the domain is insulated. In addition, the right side of the calculation domain is insulated as well.

### 2.1 Transport equations

Moisture condition contains liquid water and vapors accompanied by soils underground. Liquid water flow is displayed by Richards' equation, which represents the movement of water in unsaturated soils. In this equation, water flow $q_w$ is proportional to the product of hydraulic conductivity $K$ and gradient in water potential, where matric potential $\psi$ and local gravitational potential $gz$ are considered. The relative location $z$ is measured from the datum plane and gravitational acceleration $g$ can be considered constant.

$$q_w = -K\nabla(\psi + gz) \quad (1)$$

Vapor flow $q_v$ is derived based on Fick's law which describes the relationship between diffusion flux and concentration. Here water vapor flow is driven by a gradient in vapor concentration, which depends on the temperature $T$ and humidity $h$. The vapor flow can be calculated as the sum of temperature-driven diffusion flux $q_{v,T}$ and isothermal diffusion flux $q_{v,i}$.

$$q_v = q_{v,i} + q_{v,T} = -D_v c_v' \nabla h - D_v h s \nabla T \tag{2}$$

Where $D_v$ is vapor diffusivity, $c_v'$ saturated vapor concentration, $s$ the slope of saturated vapor concentration function curve.

Heat flow underground consists of sensible heat component, latent heat component and the convective thermal component brought by flowing water. Sensible heat flow is formulated as the Fourier's law of heat conduction, where the thermal energy flow is calculated as the product of thermal conductivity $\lambda$ and the gradient in temperature. Latent heat flow is related to the phase transition process of water vapor, accompanied by thermal energy absorbed and released into soil. It can be derived as the sum of latent heat of vaporization $L$ and heat energy in water $TC_w$, where $C_w$ is the specific heat of water.

$$q_h = -\lambda \nabla T + (L + TC_w) q_v + TC_w q_w \tag{3}$$

The continuity equation for the mass in this closed underground system states the relationship of water flow including liquid water and vapor, and the change of water content per volume $\rho_w \theta$, where $\rho_w$ is the density of water and $\theta$ the volumetric water content.

$$\rho_w \frac{\partial \theta}{\partial t} = -\nabla \cdot (q_w + q_v) \tag{4}$$

The law of conservation of energy provides the relationship between the change of temperature and thermal energy flow. In the underground thermal system, specific heat is composed of three parts, the heat in liquid water, $C_w \rho_w \theta$, the heat stored in the soil, $C_m \rho_m \chi_m$, and the heat from the air fraction, $C_a \rho_a \chi_a$. $C_m$ and $C_a$ are the specific heat of soil component and air part respectively. $\rho_m$ represents the density of soil and $\rho_a$, the density of air. $\chi_m$ and $\chi_a$ are the volumetric fractions of solid minerals and air. The change of specific heat in air part makes little contribution to the energy flow compared to the changes in liquid and solid components, own to the amount of specific heat stored in the air is so small (Kroener et al., 2014). Therefore, it can be neglected when calculating the thermal energy.

$$(C_m \rho_m \chi_m + C_w \rho_w \theta) \frac{\partial T}{\partial t} = -\nabla \cdot q_h \tag{5}$$

### 2.2 Parameter functions

Volumetric water content and hydraulic conductivity are significant properties for evaluating the underground moisture degree. Campbell G.S. displayed the relationship between hydraulic matric potential, volumetric water content, and hydraulic conductivity.

$\psi_e$ is the air entry potential, $\theta_s$ the saturated volumetric water content, $K_s$ the saturated hydraulic conductivity. And $b$ is the shape factor. The saturated volumetric water content is the maximum volume of water per unit volume of soil.

$$\theta = \begin{cases} \theta_s (\frac{\psi_e}{\psi})^{1/b}, & \psi < \psi_e \\ \theta_s, & \psi \geq \psi_e \end{cases} \tag{6}$$

$$K = \begin{cases} K_s (\frac{\psi_e}{\psi})^{2+3/b}, & \psi < \psi_e \\ K_s, & \psi \geq \psi_e \end{cases} \tag{7}$$

Humidity is the concentration of water vapor existed in the air. It is equal to the fraction of vapor concentration $c_v$ and the saturated vapor concentration $c_v'$. In addition, it is related to matric potential and temperature. Here, $M_w$ is the water molecular weight, $R$ the gas constant, and $T_k$ is temperature in Kelvin.

$$h = \exp\left(\frac{M_w \psi}{R T_k}\right) \tag{8}$$

The saturation vapor pressure curve separates the two-phase state and the superheated vapor state in the temperature-entropy chart. The term $M_w/(RT_k)$ functions the convertor from pressure to concentration in the

saturation vapor concentration curve. Therefore, it can be calculated for the slope of saturation vapor concentration curve $s$, where Δ is the slope of the saturated vapor pressure curve.

$$s = \frac{\Delta M_w}{RT_K} \tag{9}$$

In the vapor pressure curve, the Arden Buck equation provides a series of empirical correlations which combine the saturation vapor pressure and temperature of moisture air. The temperature is in Celsius.

$$e_s(T) = 0.611\exp\left(\frac{17.27T}{T+237.3}\right) \tag{10}$$

Here, the saturated vapor concentration is calculated as:

$$c_v' = \frac{e_s M_w}{RT_K} \tag{11}$$

The rate of evaporation of water into the atmosphere can determine the mutual coefficient of diffusion of water vapor and air. Water vapor diffusivity $D_v$ is related to the air in the porosity and the binary diffusion coefficient of water vapor $D_0(T,P)$, which depends on temperature and pressure.

$$D_v = D_0(T,P)\varepsilon(\chi_a) \tag{12}$$

$$\varepsilon(\chi_a) = \beta(\chi_a)^m \tag{13}$$

The factor $\beta$ is 0.9 and $m$ is 2.3. The binary diffusion coefficient of water vapor in atmosphere is shown as:

$$D_0(T_k,P) = D_0(237.15\text{K},101.3\text{kPa})\left(\frac{T_k}{273.15\text{K}}\right)^{1.75}\left(\frac{101.3\text{kPa}}{P}\right) \tag{14}$$

For the standard measurement condition, $D_0(237.15\text{K},101.3\text{kPa}) = 2.12\times10^{-5}\ \text{m}^2\cdot\text{s}^{-1}$.

### 2.3 Partial differential equations

The transport equations in 2.1 and parameter functions in 2.2 above lay the function of partial differential equations for mass conservation and energy conservation. In Eq(15) and Eq(16), there are 2 unknown parameters to be solved, matric potential and temperature.

$$\rho_w\frac{\partial}{\partial t}\theta(\psi) = \nabla\cdot(K(\psi)\nabla(\psi+gz) + D_v hc_v'\frac{M_W}{RT}\nabla\psi + D_v hs\nabla T) \tag{15}$$

$$(C_m\rho_m\chi_m + C_w\rho_w\theta(\psi))\frac{\partial T}{\partial t} = \nabla\cdot(\lambda\nabla T + (TC_w)K(\psi)\nabla(\psi+gz) + (L+TC_w)D_v hc_v'\frac{M_W}{RT}\nabla\psi$$

$$+(L+TC_w)D_v hs\nabla T) \tag{16}$$

### 2.4 Boundary conditions

The soil surface conditions and tank temperature determine the moisture and thermal energy flow at the interface of soil and atmosphere. The atmospheric temperature $T_0$ is set as 20 °C, and 7 °C is constant at the lower surface underground. The tank temperature $T_{tank}$ is fixed as 35 °C . Relative humidities of the top and bottom surface of underground domain are set as 0.99 and 0.999, respectively. The convective heat transfer coefficient between upper boundary and atmosphere $h_1$ is 0.5 W/(m$^2$·K), for that between tank and soil $h_2$ 300 W/(m$^2$·K).

The boundary conditions take the following form regarding other interfaces.

$$\frac{\partial T}{\partial x}(W,y) = 0 \tag{17}$$

$$\frac{\partial T}{\partial y}(x,-H) = 0 \tag{18}$$

$$\frac{\partial T}{\partial y}(x,0) = h_1(T-T_0) \tag{19}$$

For the tank:

$$\frac{\partial T}{\partial r}(r_i, \alpha) = h_2(T - T_{tank}) \quad (20)$$

## 3. Validation of the non-isolated tank model

In the coupled simulation model, parameters for calculating the temperature of non-insulated underground thermal storage tank and soil around are given in Table 1. As shown in Part 2, the nodes numbering used in the calculations are marked in Figure 3. Actual annual weather data from December 2020 to December 2021 was inputted into the model to obtain more precise results. The model was operated for one-year totally. Schematic of the UHSU experimental measurements is arranged in Figure 4.

The initial soil temperature around the tank, initial relative humidity of top and bottom layers underground, initial top and bottom tank temperature, along with weather data were collected in the first days of selected months to verify the coupled model. Two series of validation were conducted: verification of the top tank temperature and tank temperature.

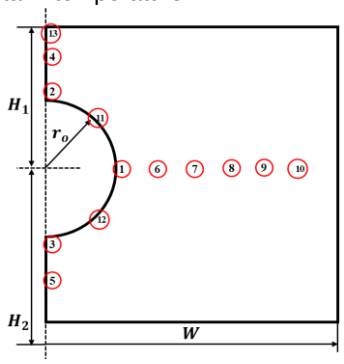


*Figure 3: Typical nodes in MATLAB simulation for modelling of the UHSU*

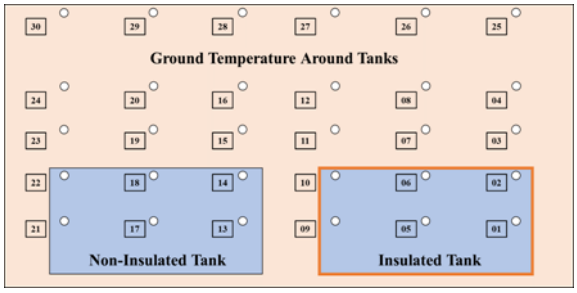


*Figure 4: Schematic of temperature sensors positions in the UHSU experiment*

*Table 1: Parameters for UHSU model in MATLAB*

| Parameter | Description | Parameter Value |
|---|---|---|
| $r_o$ | Outer radius of the tank | 1.5 m |
| $W$ | Ground width | 12 m |
| $H_1$ | Tank burial depth | 5 m |
| $H_2$ | Underground depth | 15 m |
| $h_1$ | Air-to-insulated ground heat transfer coefficient (external surface) | 0.5 W/(m$^2$·K) |
| $h_2$ | Water-ground heat transfer coefficient in the non-insulated tank | 300 W/(m$^2$·K) |
| $\rho_w$ | Water density | 1,000 kg/m$^3$ |
| $c_w$ | Water specific heat | 4,180 J/(kg·K) |
| $c$ | Ground specific heat | 1,000 J/(kg·K) |
| $\rho$ | Ground density | 1,200 kg/m$^3$ |
| $k$ | Ground thermal conductivity | 1.2 W/(m·K) |
| $A_{PV}$ | The surface area of photovoltaic PV panels | 42.66 m$^2$ |
| $\eta_{PV}$ | Thermal efficiency of PV panels | 0.45 |

For the verification of the top tank temperature, temperature recordings of node 2 in model (Figure 3) and node 14, 18 and 22 from measurements (Figure 4) were collected to compare. The results are shown in Table 2.
For the verification of average tank temperature, temperature recordings of node 1, 2, 3, 11 and 12 in model (Figure 3) and the average temperature of top and bottom layer of tank in truth measurements were utilised to validate. The results are displayed in Table 3.

*Table 2: Validation results of top tank temperature*

| Date | Temperature in model (°C) | Temperature in measurement (°C) | Relative error (%) |
|---|---|---|---|
| 2021-05-01 | 15.532 | 15.133 | 2.637 |
| 2021-09-01 | 28.227 | 28.300 | 0.258 |
| 2021-10-01 | 27.013 | 26.133 | 3.367 |
| 2021-11-01 | 20.886 | 20.200 | 3.396 |

*Table 3: Validation results of average tank temperature*

| Date | Temperature in model (°C) | Temperature in measurement (°C) | Relative error (%) |
|---|---|---|---|
| 2021-07-01 | 34.384 | 33.550 | 2.485 |
| 2021-08-01 | 34.535 | 33.600 | 2.782 |
| 2021-09-01 | 27.592 | 29.300 | 5.829 |
| 2021-10-01 | 26.591 | 27.550 | 3.479 |

From the results above, one can observe that relative error between model and experiment of the top tank temperature varies from 0.258 % (September) to 3.396 % (November) whilst it is in the range of 2.485 % (July) to 5.829 % (September) in the case of tank temperature. A possibility account for temperature discrepancy is that the simulation process considers little irreversible loss, which results in a fully heat transfer between the tank and soil in the underground occurred. Besides, the temperature in the simulation model shows the same trend with it in the actual measurement.

## 4. Conclusions

This paper presents the validation process of a coupled model between moisture and heat transfer of RESHeat underground heat storage unit. The ordinary differential equations are formulated to obtain the thermal energy balance of the underground energy storage system. Actual measurements including non-insulated thermal storage tank temperature, soil temperature, relative humidity and weather data have been initialised the proposed model. Two types of tank temperatures are analysed between the simulation and experiments. Results show that relative error of model and measurement varies from 0.258 % to 3.396 % (for top tank temperature) and from 2.485 % to 5.829 % (for average tank temperature).

### References

Daneshazarian R., Bayomy A.M., Dworkin S.B., 2022, NanoPCM based thermal energy storage system for a residential building, Energy Conversion and Management, 254, 115208.

Kroener E., Vallati A., Bittelli M., 2014, Numerical simulation of coupled heat, liquid water and water vapor in soils for heat dissipation of underground electrical power cables, Applied Thermal Engineering, 70, 510-523.

Li K., Jiang Y., Jia L., Zhao G., Kaita M., 2023, Modeling study on nearly-zero carbon cooling in single houses with underground cold storage, Journal of Energy Resources Technology, 145, 012103.

Ocłoń P., Chin H.H., Kozak-Jagieła E., Taler J., Ścisłowicz F., Czamara M., 2023, Photovoltaic–thermal waste heat integration with underground thermal energy storage and heat pump systems, Handbook of Process Integration (PI), Woodhead Publishing Limited, Cambridge, UK, 1017-1042.

Ocłoń P., Cisek P., Kozak-Jagieła E., Taler J., Taler D., 2020, Modeling and experimental validation and thermal performance assessment of a sun-tracked and cooled PVT system under low solar irradiation, Energy Conversion and Management, 222, 113289.

Ocłoń P., Ławryńczuk M., Czamara M., 2021, A new solar assisted heat pump system with underground energy storage: modelling and optimisation, Energies, 14, 5137.

Xu Y., Zeng Z., 2022, Experimental and numerical investigation on the effect of heat and moisture coupling migration of unsaturated lateritic clay for the soil thermal storage system, Energy and Buildings, 276,112499.

Zhang S., Ocłoń P., Klemeš J.J., Michorczyk P., Pielichowska K., Pielichowski K., 2022, Renewable energy systems for building heating, cooling and electricity production with thermal energy storage, Renewable and Sustainable Energy Reviews, 165, 112560.